

REAL PHOTON PHYSICS EXPERIMENTS AT JLAB USING THE HALL B  
PHOTON TAGGER

WILLIAM J. BRISCOE, CATALINA CETINA and SASHA A. PHILIPS

*Center for Nuclear Studies and Department of Physics,  
The George Washington University, Washington, DC 20052, U.S.A.*

*and*

*The CLAS Collaboration  
Thomas Jefferson National Accelerator Facility, Newport News, Virginia, U.S.A.*

Received 2 April 1999; Accepted 7 June 1999

Data on real-photon induced reactions have been taken using the Tagged Photon Facility (TPF) and the Continuous Electron Beam Accelerator Facility (CEBAF) at the Thomas Jefferson National Accelerator Facility (JLab) during the first year of running in Hall B. These data have been taken for the purpose of investigating the electromagnetic structure of mesons, nucleons, and nuclei. This report summarizes the status of these experiments.

PACS numbers: 13.60.-r, 25.20.-x

UDC 539.125, 539.17

Keywords: photonuclear reactions, photoproduction, photofission

## *1. Introduction*

Of the current theories of hadronic interactions, quantum-chromodynamics (QCD) is most successful. Models have been developed using the elements of QCD that claim to have made good inroads into the explanation of the basic properties of mesons and nucleons. Further refinements are needed in these models in order to test them on the hadronic level before any attempt can be made to apply them to nuclei. However, our current level of understanding of the basic properties of hadrons is not very well founded experimentally, with resonances being proposed for demotion or elimination within the star-rating system. It is difficult to see how one can test models of the properties of bound quark systems if these properties are yet to be accurately determined. A prime example of the state of affairs is the controversy over the  $S_{11}(1535)$ ; not only with respect to its properties, but over its existence [1]. It has been said, especially of the real-photon induced reactions, that

the data are inaccurate, incomplete and inconsistent [2]. Highly accurate measurements are needed not only for the fundamental hadronic interaction to study the basic nuclear force, but even more for the electromagnetic interaction both via real and virtual photons to study the internal structure of hadrons.

## 2. Real-photon physics at JLab

The first round of real-photon experiments using the Tagged Photon Facility at the Thomas Jefferson National Accelerator Laboratory in Newport News Virginia was broken up into several running groups, each of which included experiments with similar technical needs.

The G1 Running Group combined the following approved experiments.

i) The photoproduction of single pions [3],  $\gamma p \rightarrow \pi^+ n$  and  $\gamma p \rightarrow \pi^0 p$ . The goal of this experiment is to obtain accurate and precise differential photoproduction cross sections in order to extract photo-amplitudes, coupling constants, branching ratios and resonance parameters.

ii) The photoproduction of the  $\eta$  and  $\eta'$  [4],  $\gamma p \rightarrow \eta p$  and  $\gamma p \rightarrow \eta' p$ . The proposal here is to measure differential cross sections.

iii) The electromagnetic production of hyperons [5],  $\gamma p \rightarrow K^+ \Lambda$  and  $\gamma p \rightarrow K^+ \Sigma$ . This experiment will measure  $g_{K\Lambda N}$  and  $g_{K\Sigma N}$ , and the  $\gamma p \rightarrow K^+ \Lambda / \gamma p \rightarrow K^+ \Sigma$  ratio.

iv) A search for missing baryons [6],  $\gamma p \rightarrow \pi^+ \pi^- p$ . While experiments with single-meson final states have little chance of discovering resonances not already seen in  $\pi$ -N measurements, this experiment will determine partial wave amplitudes for  $\gamma p \rightarrow \Delta^{++} \pi^-$ ,  $\gamma p \rightarrow \pi^+ \Delta^0$ ,  $\gamma p \rightarrow \rho^0 p$  and  $\gamma p \rightarrow \sigma^0 p$  in order to find "missing" non-strange baryons.

v) The radiative decays of low-lying hyperons,  $\gamma p \rightarrow K^+ Y^*$  [7]. This experiment will study the hyperon decays  $Y^* \rightarrow \gamma \Lambda$  and  $Y^* \rightarrow \gamma \Sigma$  and to measure the branching ratios.

vi) A study of the axial anomaly [8],  $\gamma \pi^+ \rightarrow \pi^+ \pi^0$  near threshold. One hopes to obtain  $d\sigma(\gamma \pi^+ \rightarrow \pi^+ \pi^0)$  and thus the  $\gamma \rightarrow 3\pi$  amplitude  $F_{3\pi}$ .

In addition to the G1 experiments, the G5 and G6 running groups also obtained data in separate running periods. The G6 running group measures photoproduction of vector mesons at high  $t$  in order to study the region below which vector dominance is important and in which hard processes are thought to dominate [9]. The G5 experiment studies the photofission of nuclei [10]. The experiment measures the total photoabsorption cross section for C, Al, Cu, Sn, and Pb and the photofission cross section for  $^{232}\text{Th}$ ,  $^{237}\text{Np}$ ,  $^{238}\text{U}$  and  $^{235}\text{U}$ . The measurements were performed with photons in the energy range between 0.16 and 2.3 GeV, using the Hall-B photon tagger. The experiment did not require the CLAS detector and constituted the commissioning experiment of the photon tagging facility.

For heavy actinide nuclei and for photon energies above 50 MeV, the total fission probability is close to one, and therefore, a measurement of the photofission

cross section is an alternate and advantageous way to determine the total photoabsorption cross section. The fission fragments were detected using parallel-plate avalanche detectors (PPADs) built at The George Washington University Nuclear Detector Laboratory (GW).

By using the photofission method, in addition to the questions regarding the nucleonic resonances in the nuclear medium, one can also address problems related to the fission process itself. Thus, we check whether the photofissility of both uranium isotopes is consistent with unity above 1.2 GeV, is there any difference in fissility between  $^{235}\text{U}$  and  $^{238}\text{U}$  as indicated in the literature in the  $\Delta$  region, and whether the  $^{232}\text{Th}$  fissility, which is only 0.8 at 1.2 GeV, remains less than one up to 1.9 GeV.

### 3. *The Hall B tagged photon facility*

Physicists from The George Washington University, The Catholic University of America, Arizona State University, and Georgetown University joined forces to design, construct and commission instrumentation for Hall B to be used in experiments concerned with real-photon induced events. This Tagged Photon Facility (TPF) is now in use at the Thomas Jefferson National Accelerator Facility. While the CEBAF large-acceptance spectrometer (CLAS) is the primary instrument to be supported by TPF, some of the early data come from two experiments which use special instrumentation in conjunction with TPF. One of these experiments [10] is described in this presentation, while the other [11] as well as CLAS itself are described elsewhere [12].

The tagging technique used for measuring the photon energy is well established. However, the JLab design represents a large increase in the photon energy range, while retaining excellent resolution. A significant feature of this system is the use of an Elbek-type electromagnet, designed and fabricated to meet the physics needs of the Hall-B facility. This 75 ton magnet has a full-energy radius of curvature of 11.80 m and deflection angle of 30 degrees. It is 6.06 m in length with a gap width of 6.0 cm.

This system is shown in Fig. 1. Electrons from CEBAF strike a thin radiator upstream of the tagger magnet. A portion of these electrons undergo bremsstrahlung while passing through a radiator which is thin enough so that electrons emit mostly a single bremsstrahlung photon. The photon energy is then determined by measuring the degraded momentum of the electron. A photon that is produced in the radiator continues along the beam line and strikes the target for the nuclear and subnuclear photoreactions to be studied in the experiment. The field setting of the tagger magnet is matched to the incident beam energy so that those electrons that do not radiate follow an arc just inside the curved edge of the pole gap and are then directed into a beam dump beneath the floor of Hall B. Bremsstrahlung electrons with energy loss between 20 to 95% of their initial energy experience a greater curvature and are detected in the focal-plane detection system, a scintillator hodoscope installed along the focal plane of the tagger magnet which lies about 2 cm

downstream of and parallel to the exit of the tagger vacuum box. The focal-plane hodoscope is segmented into 384 one-third overlapping counters in order to obtain an energy resolution of about 0.1%. The electrons exit the vacuum through a thin window located as close as possible to the detection hodoscope in order to minimize multiple scattering.

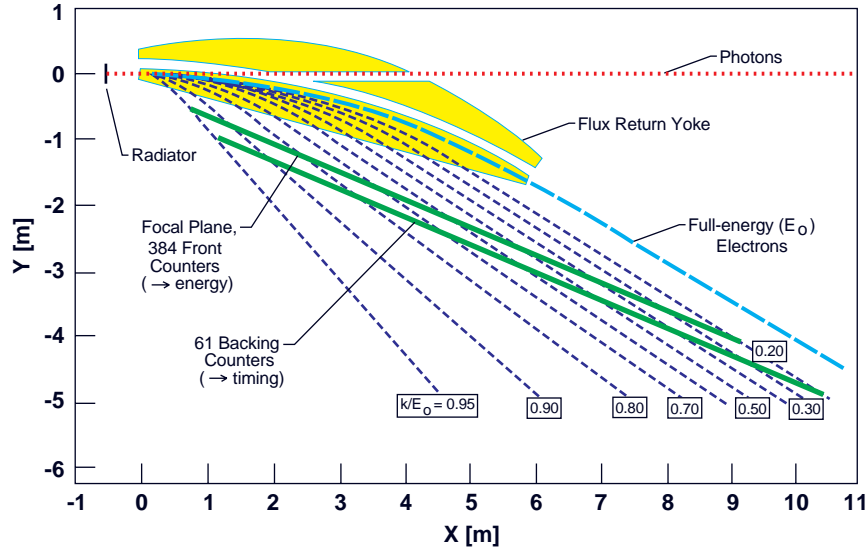


Fig. 1. The Hall B tagger at Jefferson Lab.

The tagger instrumentation provides information on the momentum and timing for each detected electron with sufficient precision to determine the photon energy to about 0.1% and to permit the forming of coincidences with interactions induced by the photon. The first of these requires a fairly high degree of segmentation, and hence demands scintillators that are quite small in one transverse dimension. The latter calls for output pulse shapes that allow precise timing, and hence for scintillators which are thick enough to ensure sufficient light for this purpose. The focal-plane instrumentation consists of two separate planes of scintillator detectors. Each detector element is oriented with its working surface normal to the local beam trajectory in "Venetian blind" geometry. The two separate planes provide for additional noise suppression capability through the use of appropriate logic circuitry to establish geometric constraints on the trajectories of detected particles. The first layer, used only for momentum definition, lies on the magnet focal surface and contains 384 narrow scintillators. The second layer lies 20 cm behind the first and contains 61 scintillators of considerably larger dimensions which are much more fully instrumented to provide the timing precision needed for the coincidence with CLAS. Electron trajectories cross these planes at angles ranging from  $9.5^\circ$  to  $25^\circ$ , and hence the optical lever arms from plane to plane along the trajectory range from about 40 to about 120 cm. The entire detector hodoscope resides inside a light-tight enclosure that is suspended beneath the tagger vacuum box.

#### 4. *Commissioning*

During the period between May 1997 and May 1998 the Hall-B photon tagger went through a commissioning period, most of which occurred in conjunction with the two experiments which use the tagger but not CLAS. Photon beams from 1.8 to 4.0 GeV were used during the commissioning period. These values were determined more by the needs of the experiments rather than consideration of tagger parameters. In all cases, tagger commissioning was done without photon beam collation in order to be able to measure the full bremsstrahlung beam during tagging efficiency measurements.

While the tagging efficiency is usually measured with a total absorption counter, during the commissioning we used two different total absorption shower counters (TASCs), one especially built for this system which is positioned just prior to the normal Hall B electron-beam-dump tunnel, and one provided by the photofission experiment which was located at the exit of the second-collimator vacuum box. The former is a set of four, 10 cm x 10 cm x 16 radiationlength (rl) Pb-glass counters while the later is a single 10 cm x 10 cm x 16 rl Pb-glass counter. Using the upstream TASC, we obtain a photon tagging efficiency of close to 99%. A lower tagging efficiency was obtained with the downstream TASC. However, these lower values are consistent with beam losses in the 30 m between the tagger radiator and the downstream TASC. That is in air, target, beam pipe windows, and in the pair spectrometer and pair-counter converters.

The link between the measure of tagging efficiency at low rates and that at nominal data-taking beam rates is done through comparison among the TASC, pair counter (PC) and pair spectrometer (PS). The latter devices are always in the photon beam just upstream of TASC. A comparison is made among these devices at lower rates and then TASC is removed. As the beam intensity is increased, the ratio of the sum of the individual T-counter scalars to PC and PS is monitored and found to be linear.

#### 5. *Down stream devices*

Several downstream devices (DSD) are used to measure and monitor the photon flux. The most reliable and direct measurement is accomplished with a set of four 16 rl x 10 cm x 10 cm lead-glass detectors called the total-absorption shower counter (TASC). This detector is used only at low rates and is not in the photon beam during data run. It has a close to 100% detection efficiency and is the main absolute measure of the photon flux and thus, when compared to the sum of all tags in the photon tagger focal plane, yields the photon tagging efficiency. Since the detector can not handle photon beam rates higher than 100 kHz, TASC is cross calibrated with two other devices, PS and PC.

The pair counter is intended as a backup intensity monitor, to be used with the full beam. The efficiency of this device for converted photons is high and it is in the beamline at all times. A thin converter produces electron-positron pairs, that are detected in coincidence between the overlap scintillator and a second layer of four

scintillators. A veto scintillator is located upstream of the converter to eliminate background coming from CLAS. The efficiency of PC is roughly 1.5 %, which leads, with a beam intensity of  $5 \times 10^7$  photons/second, to a detection rate of 1 MHz. This device is also used as a beam-position monitor, thanks to the duplication of the second layer of the coincidence system into four scintillators, which allows discrimination of the pairs produced in the right or left and in the top and bottom part of the beam.

The pair spectrometer consists of a magnet and four sets of double-ended counters, two on each side of the beam line. A photon impinging on a thin (1% rl) radiator produces  $e^+e^-$  which are detected in the symmetrically positioned counters. This device is designed to operate at the high photon beam flux,  $5 \times 10^7$  photons/second of the Hall B facility.

### 6. Preliminary results of commissioning runs

While one may not at this time be able to show anything which can come close to a cross section, there are very clear indications that the tagger and CLAS are working with sufficient reliability so that there is a good indication that good results will be obtained with sufficient time put into the analysis process. What we can show here are some preliminary figures which indicate that we are able to identify particles and obtain missing-mass and invariant-mass histograms.

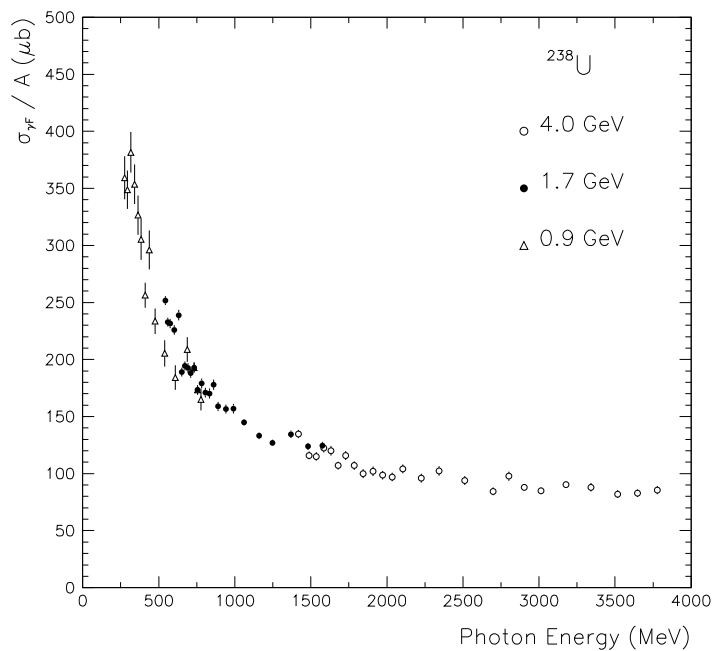


Fig. 2. The absolute photofission cross section for  $^{238}\text{U}$  divided by the mass number versus the incident photon energy for three incident electron energies (4.0, 1.7 and 0.9 GeV).

Figures 2 and 3 show some preliminary photofission (G5) measurements. For the  $^{238}\text{U}$  isotope, Fig. 2 shows the absolute photofission cross section divided by the mass number as a function of the incident photon energy, covering the range from 270 MeV to 3.8 GeV, with three incident electron energies (4.0, 1.7, and 0.9 GeV). We notice that the cross section does not show any prominent structure above the delta resonance region and that the three data sets match on smoothly with each other.

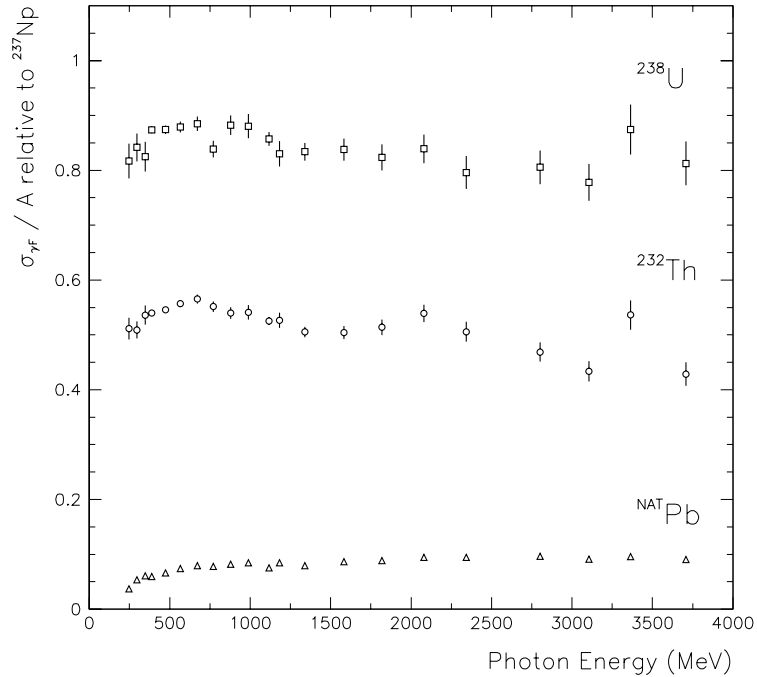


Fig. 3. The photo-fission cross sections per nucleon for  $^{238}\text{U}$ ,  $^{232}\text{Th}$ , and  $^{\text{Nat}}\text{Pb}$  divided by the  $^{237}\text{Np}$  cross section per nucleon.

Out of the six nuclei studied in this experiment,  $^{237}\text{Np}$  shows the highest photofission cross section per nucleon. Using this as a reference, in Fig. 3 we plot the cross sections per nucleon for  $^{238}\text{U}$ ,  $^{232}\text{Th}$ , and  $^{\text{Nat}}\text{Pb}$  divided by the  $^{237}\text{Np}$  cross section per nucleon. The important aspect here is the fact that the  $^{238}\text{U}$  photofission cross section is about 20% lower than that for  $^{237}\text{Np}$ . This contradicts the assumption that the fission probability for the uranium and transuranic isotopes is approximately equal to one for incident photon energies above about 50 MeV. It implies that, besides fission, there are other competing processes taking place when a few-GeV photon interacts with an actinide target. One can also tell that for thorium and lead, the values of the relative cross sections (approximately 50% and 10% respectively) scale with the fissility parameter  $Z^2/A$ .

For the G1 and G6 commissioning runs, we show Figs. 4a-d. These plots show the first identification of the  $\gamma p \rightarrow p + 2\pi^0$  channel [12] with CLAS. Figure 4a shows

the missing mass of  $\gamma p \rightarrow pX$ ; Fig. 4b shows the same as Fig. 4a but only selected events that are above the two-pion threshold of 270 MeV; Fig. 4c shows the invariant mass of two photons detected in the electromagnetic calorimeters for those events that have exactly two neutrals in them; and Fig. 4d shows those events that are above the two-pion threshold and lie between 128 and 142 MeV in Fig. 4c and thus the two photons emanate from a  $\pi^0$ . Figure 4d is actually the missing mass squared of  $\gamma p \rightarrow p + \pi^0 + X$ , and the peak identifies the second  $\pi^0$ . Again no

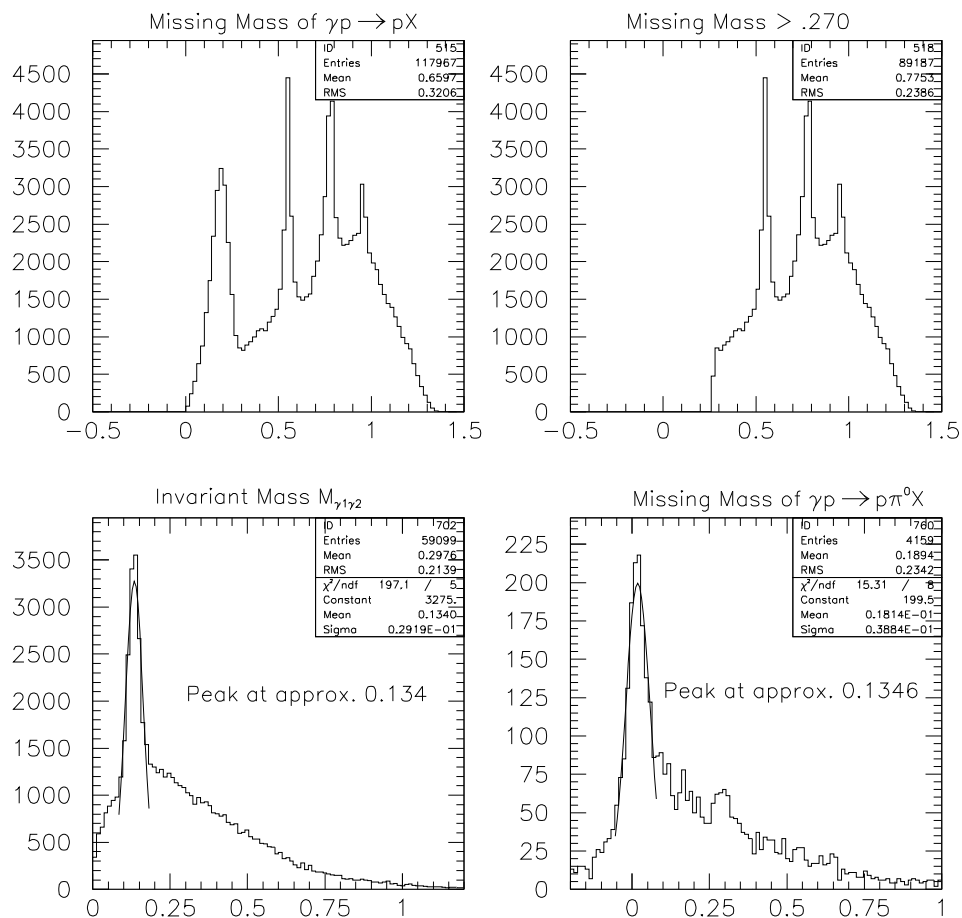


Fig. 4. The first identification of the  $\gamma p \rightarrow p2\pi^0$  channel with CLAS. a) the missing mass of  $\gamma p \rightarrow pX$ ; b) events above the two-pion threshold; c) the invariant mass of two photons detected in the electromagnetic calorimeters for events with exactly two neutrals; and d) events above the two-pion threshold with two photons emanating from a  $\pi^0$ . Figure d) shows the missing mass squared of  $\gamma p \rightarrow p\pi^0 X$ ; the peak identifies the second  $\pi^0$ .

attempt is made here to draw any conclusion other than the optimistic view that, having clearly identified the  $\gamma p \rightarrow p2\pi^0$  reaction, we expect that good things will come from a strong analysis effort.

## 7. Conclusion

The JLab Hall B facility is now complete and has taken its first real-photon beam. The tagged photon facility is operational and works close to expectations. Data have been taken both with and without CLAS and a strong analysis effort is underway. We expect that first cross sections will be forthcoming from the data soon.

### References

- 1) G. Höhler, *Proceedings of the 8th International Workshop in N\* Physics*, W. J. Briscoe, H. Haberzettl and C. Bennhold, eds.,  $\pi$ -N Newsletter **14** (1998); <http://www.gwu.edu/~cns/nstar.htm>;
- 2) R. Arndt, private communication;
- 3) *The Photoproduction of Single Pions*, spokespersons: W. J. Briscoe, D. Jenkins and J. Ficenic; [http://www.cebaf.gov/exp\\_prog/CEBAF\\_EXP/E94103.html](http://www.cebaf.gov/exp_prog/CEBAF_EXP/E94103.html);
- 4) *Photoproduction of the  $\eta$  and  $\eta'$* , spokesperson: B. Ritchie and M. Dugger; [http://www.cebaf.gov/exp\\_prog/CEBAF\\_EXP/E91008.html](http://www.cebaf.gov/exp_prog/CEBAF_EXP/E91008.html);
- 5) *Electromagnetic Production of Hyperons*, R. Schumacher and J. McNabb; [http://www.cebaf.gov/exp\\_prog/CEBAF\\_EXP/E89004.html](http://www.cebaf.gov/exp_prog/CEBAF_EXP/E89004.html);
- 6) *A Search for Missing Baryons Formed in  $\gamma p \rightarrow \pi^+ \pi^-$  using CLAS at CEBAF*, J. Napolitano and M. Klusman; [http://www.cebaf.gov/exp\\_prog/CEBAF\\_EXP/E93033.html](http://www.cebaf.gov/exp_prog/CEBAF_EXP/E93033.html);
- 7) *Radiative Decays of Low-Lying Hyperons*, G. Mutchler and S. Taylor; [http://www.cebaf.gov/exp\\_prog/CEBAF\\_EXP/E89024.html](http://www.cebaf.gov/exp_prog/CEBAF_EXP/E89024.html);
- 8) *Study of the Axial Anomaly Using the Reaction  $\gamma \pi^+ \rightarrow \pi^+ \pi^0$* , R. A. Miskimen, K. Wang, A. Yegneswaren and B. Asavapibhop; [http://www.cebaf.gov/exp\\_prog/CEBAF\\_EXP/E94015.html](http://www.cebaf.gov/exp_prog/CEBAF_EXP/E94015.html);
- 9) *Photoproduction of Vector Mesons at High  $t$* , M. Anghinolfi, J. Laget, C. Marchand and E. Anciant; [http://www.cebaf.gov/exp\\_prog/CEBAF\\_EXP/E93031.html](http://www.cebaf.gov/exp_prog/CEBAF_EXP/E93031.html);
- 10) *Photoabsorption and Photofission of Nuclei: TJNAF Experiment 93-019*, N. Bianchi, V. Muccifora and B. L. Berman, GW thesis experiment for C. Cetina; The photoabsorption portion of this experiment was accomplished elsewhere during Hall B construction and not repeated at JLab; [http://www.cebaf.gov/exp\\_prog/CEBAF\\_EXP/E93019.html](http://www.cebaf.gov/exp_prog/CEBAF_EXP/E93019.html);
- 11) *A Measurement of Rare Radiative Decays of the Phi Meson*, spokespersons: A. Dzierba and J. Napolitano; [http://www.cebaf.gov/exp\\_prog/CEBAF\\_EXP/E94016.html](http://www.cebaf.gov/exp_prog/CEBAF_EXP/E94016.html);
- 12) L. Cole Smith, *Fizika B (Zagreb)* **8** (1999) 1;
- 13) *Analysis of the Contribution from the  $\gamma p \rightarrow p2\pi^0$  Reaction Channel*, S. Philips and B. L. Berman.

MJERENJA U JLAB S REALNIM FOTONIMA POMOĆU FOTONSKOG  
OZNAČIVAČA U DVORANI B

Tijekom prve godine rada sustava s označavanjem fotona u dvorani B pri ubrzivaču s neprekidnim elektronskim snopom (CEBAF) u Thomas Jeffersonovom nacionalnom akceleratorском pogonu (JLab) postigli su se podaci o raznim fotonima izazvanim reakcijama. Tim se podacima istražuju elektromagnetske strukture mezona, nukleona i atomskih jezgri. Ovaj je rad sažetak tih mjerenja.